Lung Cancer Nodule Detection Using Convolutional Neural Networks

Jay Joshi

M.S Information Securtiy, California State University Los Angeles

Abstract- Cancer being a disease which might be cured if detected in early stage makes it vital to enhance the techniques for detection. Currently, pulmonic cardiologists use some CAD systems to notice malignant respiratory organ nodules in chest radiographs. Within the past years the advancements in Convolutional Neural Network models have improved image classification and detection however it's not nevertheless be ran down to an excellent extent in detection of respiratory organ nodules in chest radiographs. In this paper, we propose a brand new framework of ensemble of convolutional neural networks and use it to considerably to cut back the quantity of false positive on respiratory organ nodules detection in chest radiographs (CXR). Firstly, the raw pictures square measure increased victimization un-sharp mask technique. Then, we have a tendency to cut the improved pictures into patches of pictures containing or not containing nodule from enhanced CXRs, that corresponds to the positive and negative samples. Third, three CNNs having totally different input size and depths square measure created to notice respiratory organ nodule individually. Finally, a logical AND operator is employed to fuse the results of the three CNNs and E-CNNs square measure created for respiratory organ nodule detection.

Index Terms- Lung Nodule, Convolutional Neural network, Lung cancer, Radiograph processing, Feature Extraction, Sensitivity, Computed Tomography.

I. INTRODUCTION

Lung cancer is one of the leading causes of deaths globally with 14 million new cases and 8.2 million deaths among other infectious and cardiac disease. In the United States of America around $125 billion have been utilized for cancer cure and can even rise to $156 billion by 2020. Below is a graph of incidences and mortality rate due to lung cancer in some developed countries.

Figure-2 shows the deaths due to lung cancer with respect to other cancers like stomach, oral or liver etc. which can spread much rapidly because of imbalanced living measures or inappropriate medication.
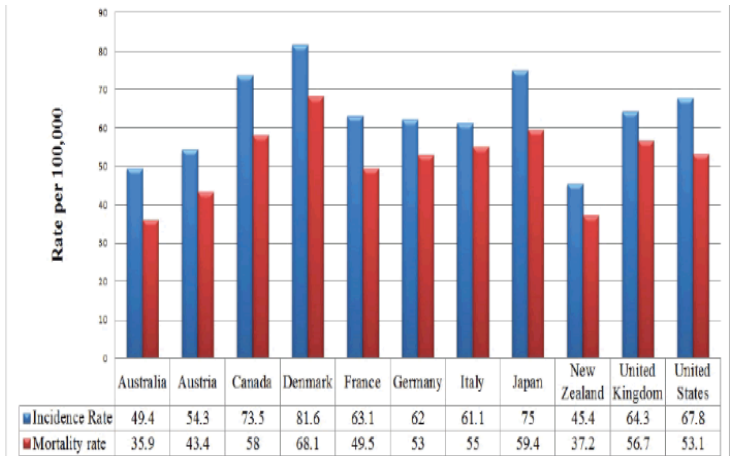

Figure-1 Incidences and Mortalities due to lung cancer in some developed nations.
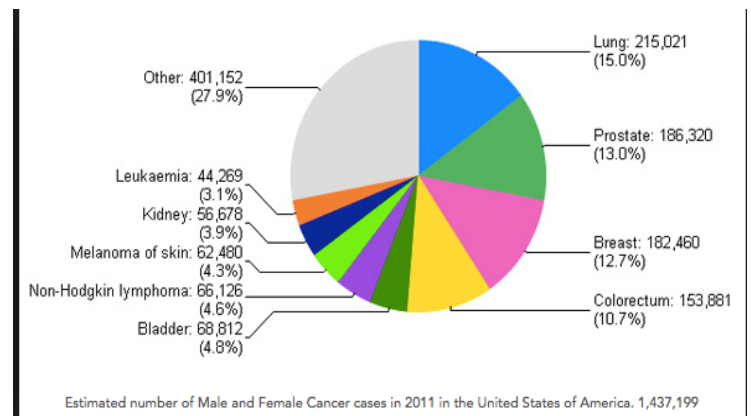

Figure-2 Lung cancer cases with respect to other types of cancer

In order, to decrease this numbers and decrease the casualties due to lung cancer it becomes important to develop a method to detect lung cancer at an early stage as treatment at early stage is possible improving a person's survival chances as compared to a person in later stages. Thus it becomes very important to find an effective way to detect lung cancer at an early stage. Medical professionals use TNM classification to help characterize lung cancer from basic to advanced forms of malignant tumors. IA being the earliest stage of cancer, which is more likely that it was accidentally discovered, the more difficult it will be to perform a biopsy and ultimately the better the prognosis. On the other hand,

IV is an advanced stage of cancer, which means that it is easier to diagnose, including biopsy, highly likely to cause symptoms and the worse prognosis.

Table 1.1 shows the TNM7 Lung Cancer classification diagnosis in 2016. The majority of people that are diagnosed already have reached the most advanced stage of lung cancer (IV). The second majority are in the earliest classification, according to Dr. Linnane at Beaumont Hospital this group had accidentally been diagnosed with lung cancer while taking a CT Scan for another problem.

TNM 7 Classification	No. of Patients
IA	214
IB	72
IIA	53
IIB	64
IIIA	139
IIIB	71
IV	368
Total	981

Table 1.1- TNM7 Classification Count in Beaumont Hospital 2016.

A main problem medical professionals face while dealing with IA lung cancer is that the tumor is so small i.e. less than 4mm that it is very difficult to know whether it is benign or malignant and it would be too early to suggest biopsy so they have to wait for 6-12 weeks and than do the CT scan to see the growth of the tumor. Another problem they face is known as observer's fatigue, according to Krupinski et al, after a day of clinical reading, radiologists have reduced ability to focus, increased symptoms of fatigue and oculomotor strain and reduced ability to detect fractured and further continues to say that radiologists need to be aware of the effects of fatigue on diagnostic accuracy and take steps to mitigate these effects.

Along with CT scan another technique used in a similar way is a basic X-ray imaging. Though CT scan is considered to be the most effective imaging method for lung nodule detection at an early stage yet, it is expensive and often not available in low-level hospitals. On the other hand, the basic chest radiographs are most cost-effective, dose-effective and routinely available diagnostic tool, so CXRs is the first diagnostic step for detecting any chest abnormalities. On making some improvements in already existing techniques using CXRs lung nodule detection at early stage can become more effective.

A chest radiograph is not easy to interpret as it has complicated superimposed anatomical structure. It becomes difficult even for experienced radiologists to distinguish infiltrates from the normal pattern of branching blood vessels in the lung fields, or detecting subtle nodules that indicate lung cancer. Thus, it is necessary to develop computer algorithms to assist radiologists in reading CXRs.

II. RELATED WORK

Since long work is done on computer-aided diagnosing (CAD) system for respiratory organ nodule detection, that is done to create the identification of respiratory organ nodules faster and a lot of correct. Mastsumoto et al show that it cannot facilitate the doctors to enhance diagnostic accuracy, albeit CAD system gets the sensitivity over eightieth at the false positive per image level of eleven. Ahmad et al. performed experiments on JSRT by taking traditional and abnormal pictures of equal range and determined 2 region of interest from every image and applied texture operate together with a fisher constant to spot best options. Keserci and Yoshida use edge target-hunting riffle snake model to extract the sting of rib and nodule edge coverage feature then scale back the false positive rate by mistreatment this feature and alternative morphological options.

Orban et al. worked on to process the skiagraph pictures to get rid of the ribs associated collar bone from the respiratory organ pictures to reinforce the detection rate by applying strained slippy band filter for intensity live with Support Vector Machine (SVM) on appropriate matter options and scored sixty one sensitivity by minimizing doable false alarms whereas an accuracy of eighty three was achieved with neural network by group action with entropy and energy base feature process techniques. Penedo et al. gift a two-level artificial neural specification to reinforce respiratory organ nodules in CXRs. Suzuki et al. developed a multi-resolution huge coaching artificial neural network image process technique that helps suppress the distinction of ribs and clavicles in CXRs. They use "virtual dual-energy" technique to boost the sensitivity.

Along with designation growth from respiratory organ nodule few researchers have additionally worked with respiratory organ lesions from chest radiographs by integration matter and mensuration primarily based techniques for attribute process along side effective classification. Enhancing the image quality by modifying specific attributes victimization abstraction domain algorithms that eliminates unsuitable details of the image along side noise and will increase brightness by applicable resizing and filtering to own higher image quality for clinical apply.

Since few years, because of fast development of deep learning, convolutional neural network has created huge progress, particularly in image classification and object detection. The advantage of CNN is that it will extract options mechanically by exploitation massive amounts of knowledge to get higher results. Weight sharing and back propagation algorithmic program will

facilitate the model get a more robust generalization performance and world optimum.

Some other methods are also being used for enhancing sharpness, equalizing histogram without harming the radiographs sensitivity and achieve better results.

III. MATERIALS AND METHODS

A. Image Dataset

Our primary dataset is the dataset provided by Japanese Society of Radiological Technology (JSRT). The CXRs in the database were collected from 14 medical institutions by using screen-film systems over a period of 3 years. CT confirmed all the nodules in the CXRs, and the three chest radiologists who were in complete agreement confirmed the locations of the nodules. Overall it includes 247 chest radiographs among which 100 are malignant, 54 are benign and 93 are normal X-ray images. These images were digitized to yield 12-bit CXRs with a resolution of 2048 * 2048 pixels. The size of pixel was 0.175 * 0.175 mm. Figure-3 provides the distribution of abnormal cases among male and female.

JSRT Cancer Nodule Cases

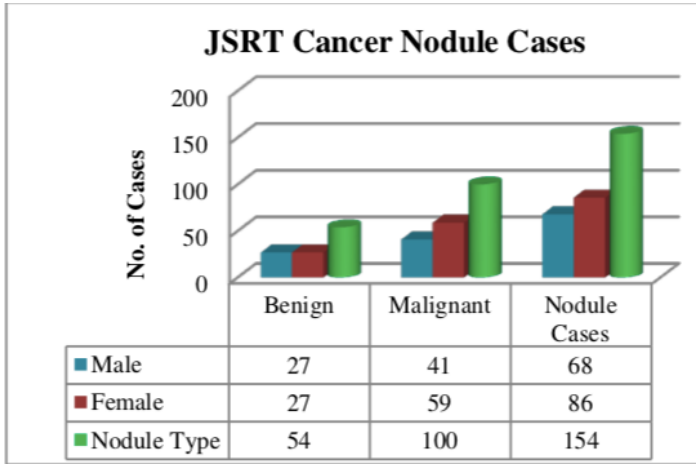|	Benign	Malignant	Nodule Cases
■ Male	27	41	68
■ Female	27	59	86
■ Nodule Type	54	100	154

Figure-3 Gender wise distribution of JSRT cancer cases.

For simplicity purposes we can further re-divide the nodules into two classes for the experiments: 'practicable' for obvious, relatively obvious, subtle cases and 'hard' for very subtle and extremely subtle cases, as listen below in Table 3.1

	size			total
	Small	Medium	Large	
Extremely subtle	2	18	5	25(16.2%)
Very subtle	3	16	10	29(18.8%)
Subtle	4	29	17	50(32.5%)
Relatively obvious	1	20	17	38(24.7%)
Obvious	0	5	7	12(7.8%)
hard	**5**	**34**	**15**	**54(35.1%)**
practicable	**5**	**54**	**41**	**100(64.9%)**

Here we propose a new method of ensemble of convolutional neural networks (E-CNNs) to directly detect lung nodules, which omits the lung field segmentation procedure, and avoids the loss of true lung nodules while extracting the features.

Table-3.1 The Distribution of Lung Nodules in the JSRT

In figure-4 we display some nodule and non-nodule patches, which the circles demonstrate the location and the size of the nodule given by JSRT. It can be seen that the nodule and non-nodules are very different to be distinguished if without the ground truth especially for hard group.
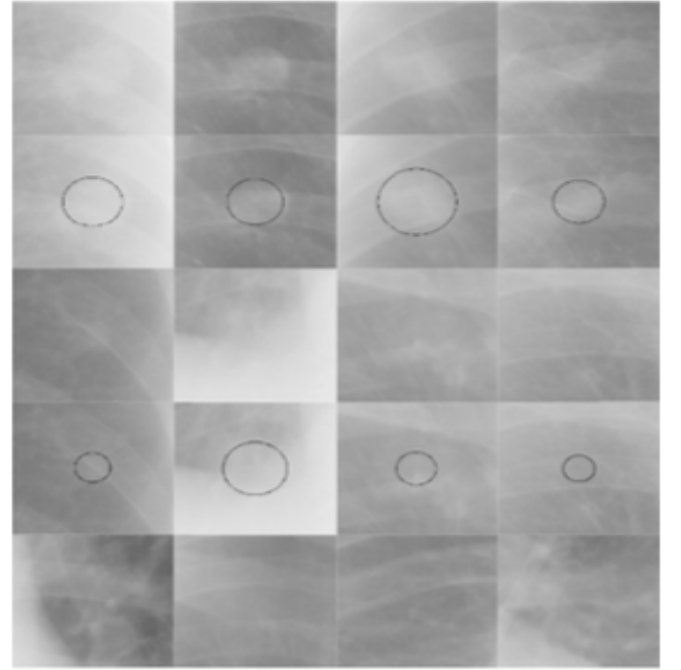

Figure-4 some nodule and non-nodule patches. 1st row is practicable cluster and also the second row is ground truth of 1st row and also the third row is tough cluster and also the fourth row is that the ground truth of the third row and also the last row is non-nodule patches.

B. CNN for Lung Nodules Detection

The whole procedure of CNN for detecting lung nodules is as below:
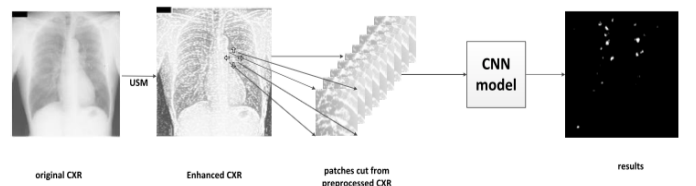
a) Image Preprocessing:

Data preparation needs to be applied to all or any pictures. It will be finished either of the subsequent 2 methods:

Firstly, we are able to use Unsharp Mask (USM) image sharpening technique to reinforce the nodule signal within the CXRs. The equation that may be used for identical is:

$$I_s = I_o + (I_o - I_b) * Amount$$

where I_s denotes the sharpened image and therefore the I_o denotes the initial image and I_b is that the blurred image, and quantity denotes what proportion distinction is supplemental at the perimeters. Here we will use the mathematician Blur technique to blur image and set quantity to fifty. The result of this would be something like in the figure below.
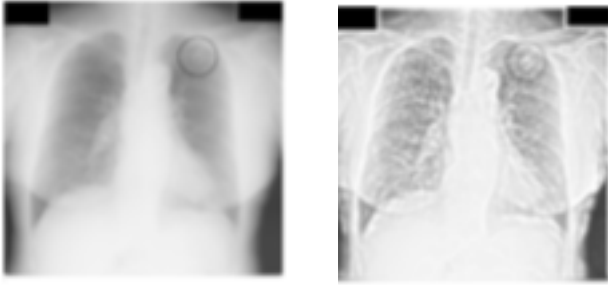

Figure 5(a) Original Image   Figure 5(b) Enhanced Image

Another method that can be used enhance the images consists of the following 4 steps:

- Step-1: Increasing the contrast of all images using Histogram Equalization. This allows normalizing the intensity of images from the dataset.

- Step-2: Removing the noise from the images using Median Filtering with a window size of 3*3.

- Step-3: Resizing images to 224 * 224 pixels to match the input of the model used in this study.

- Step-4: Normalizing image color based on mean and standard deviation of the ImageNet training set.

b) CNN Architecture Construction:

The CNN may be a extremely nonlinear filter that may be trained by mistreatment input pictures and therefore the corresponding teaching labels. It invariably consists of multi convolutional layers, pooling layers and totally connected layers. The basic architecture of our proposed CNN for detection of lung nodules is shown in figure 6:
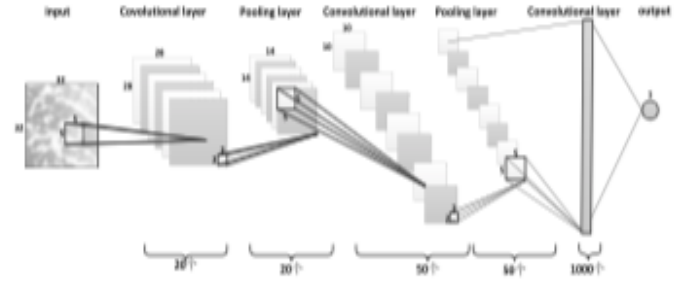

Figure-6: Proposed CNN Architecture

Here we input images that are 32*32 patches cut from the enhanced CXRs.

c) Convolutional Layer and Pooling Layer:

The convolutional layer extracts pictures options victimization convolutional calculation with completely different convolutional kernels. every kernel convolves the input to output a sort of feature. This configuration simulates the native perception characteristics of human sensory system. during this computation, activation operate is extremely necessary. Rectified Linear Units (ReLU) is wide used as activation operate within the fresh planned CNN models. Study from Krizhevsky et al. incontestable that ReLUs change the network to coach many times quicker than victimization tanh units in deep CNN. The equation is as following:

$$f(x) = max (0, \sum w_i \alpha_i)$$

where $\mathbf{w}$ is the connection weights, and $\boldsymbol{\alpha}$ is the output from the formal layer.

Here, we use linear activation function in the first and second convolutional layers, and ReLUs function in the third convolutional layer and the last fully connected layer.

d) Training:

We train our network from scratch on patches taken from large images. By taking small patches as input, much larger number of training samples are gained, which meet the needs of CNNs. For training the whole model, the loss function is defined as follows:

$$\mathcal{L} = \tfrac{1}{2} \| f(w;x) - y \|^2$$

where x is the input patch, and w are weights for each layer, and f is the candidate predict function. y denotes whether the input patch contains a true lung nodule, and 1 for yes and 0 for no. The back-propagation and stochastic gradient descent (SGD) methods are used to train the weights as follows:

$$w` = min` \mathcal{L}$$

$$\Delta w = \nabla_w \mathcal{L}$$

$$w = w + \alpha \Delta w$$

C. Ensemble of CNNs (E-CNNs) for Lung Nodules Detection

a) Algorithm Introduction

The similarities to different scales of patches are different. As shown is figure 7, even if it is subsampled from original patches, and can still be recognized as containing nodules. But those similar to be the subsampled patches known as false-positives are different. So in this paper, we propose an ensemble model of CNNs to reduce false positives.
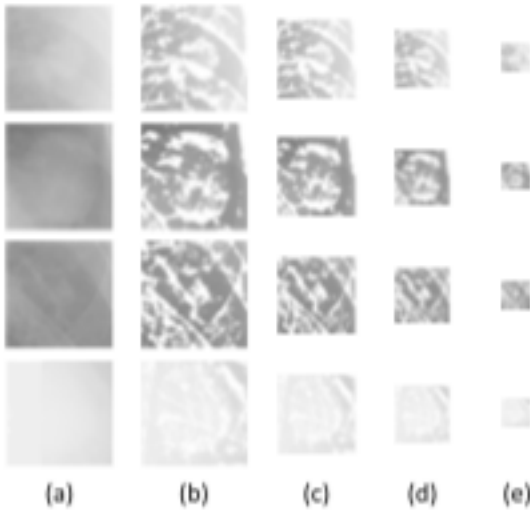

Figure-7: Nodule patches of different scales. (a) the raw patches, (b) the USM enhanced patches, (c) 60 * 60 patches, (d) 32*32 patches, (e) 12*12 patches

One single CNN has limited learning capacity, and may not learn all the essential features to distinguish a nodule from various types of non-nodule structure, but multi different CNNs can deal with much more non-nodules. So we propose the Ensemble of CNNs (E-CNNs) to reduce the false-positive.

Different Architectures of CNN can deal with different input images. With different scales of subsample of the patches, our proposed E-CNNs model deal with the non-nodule patch differently. When they all can mark the true positive (TP), we can reduce the false positives by a complete agreement.

b) Architecture of E-CNNs

Here we construct 3 CNNs for different input scales, i.e. CNN1, CNN2 and CNN3, and their architecture is shown in Table-3.2.

The architecture of proposed E-CNNs is shown in figure-8 and a logical AND operator is used to fuse the results of CNN1, CNN2 and CNN3. An example of results of using different CNN is shown in figure-9, which demonstrates lots of false-positives are reduced by using the E-CNNs compared figure-9 (a),(b),(c) with figure-9(d).
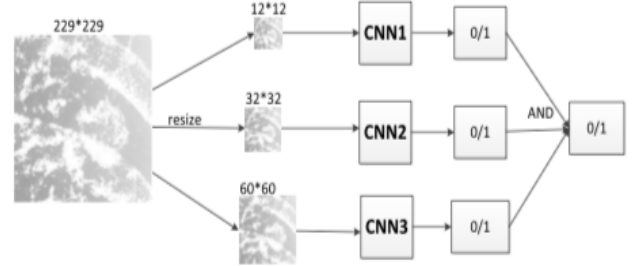

Figure-8 The architecture of the ensemble of CNNs

Layer	Type	Input	Kernel	Stride	Pad	Output
(a) CNN1						
0	Input	12×12	N/A	N/A	N/A	12×12
1	Convolution	12×12	5×5	1	0	$20 \times 8 \times 8$
2	Max pooling	$20 \times 8 \times 8$	2×2	2	0	$20 \times 4 \times 4$
3	Convolution	$20 \times 4 \times 4$	4×4	1	0	1000×1
4	Fully Connected	1000×1	1×1	1	0	1×1
(b) CNN2						
0	input	32×32	N/A	N/A	N/A	32×32
1	Convolution	32×32	5×5	1	0	$20 \times 28 \times 28$
2	Max pooling	$20 \times 28 \times 28$	2×2	2	0	$20 \times 14 \times 14$
3	Convolution	$20 \times 14 \times 14$	5×5	1	0	$50 \times 10 \times 10$
4	Max Pooling	$50 \times 10 \times 10$	2×2	2	0	$50 \times 5 \times 5$
5	Convolution	$50 \times 5 \times 5$	5×5	1	0	1000×1
6	Fully Connected	1000×1	1×1	1	0	1×1
(c) CNN3						
0	input	60×60	N/A	N/A	N/A	60×60
1	Convolution	60×60	5×5	1	0	$20 \times 56 \times 56$
2	Max pooling	$20 \times 56 \times 56$	2×2	2	0	$20 \times 28 \times 28$
3	Convolution	$20 \times 28 \times 28$	5×5	1	0	$50 \times 24 \times 24$
4	Max pooling	$50 \times 24 \times 24$	2×2	2	0	$50 \times 12 \times 12$
5	Convolution	$50 \times 12 \times 12$	5×5	1	0	$100 \times 8 \times 8$
6	Max pooling	$100 \times 8 \times 8$	2×2	2	0	$100 \times 4 \times 4$
7	Convolution	$100 \times 4 \times 4$	4×4	1	0	1000×1
8	Fully Connected	1000×1	1×1	1	0	1×1

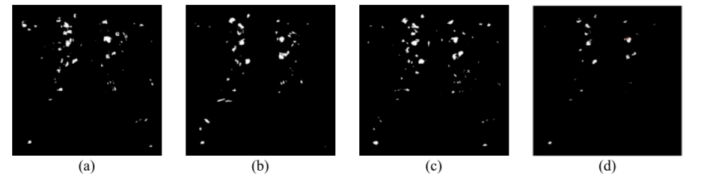Table-3.2 The CNN architectures used in our experiments

Figure-9 Results using CNN, (a) Results of CNN1; (b) Results of CNN2; (c) Results of CNN3; (d) Results of E-CNNs.

IV.   RESULTS AND CONCLUSION

The performance of the model during this study was evaluated victimization accuracy, specificity, and sensitivity. The accuracy shows the degree to that the model properly known each positive and negative cases. The specificity shows the degree to that the

model properly known negative cases and sensitivity shows the degree to that the model properly known positive cases. By having high accuracy, specificity and sensitivity, it are often tacit that the model has low error. The accuracy we tend to get from the planned model is 85.5%.

To conclude, the performance of the densely connected convolutional network on detective work carcinoma from chest x-ray pictures was explored. Since the dataset was too tiny to coach the convolutional neural network, was projected a method to coach the deep convolutional neural network employing a terribly tiny dataset. The strategy was to coach the model many times, having the model study the ultimate task step-by- step, that during this case, starts from the utilization of general pictures within the ImageNet dataset, followed by characteristic nodules from chest x-rays in ChestX-ray14 dataset, and at last characteristic carcinoma from nodules within the JSRT dataset.

REFERENCES

W. H. Organization, "Cancer," 2018. [Online]. Available: http: //www.who.int/mediacentre/factsheets/fs297/en/

[2] C. Zwirewich, S. Vedal, R. R Miller, and N. L Mller, "Solitary pulmonary nodule: high-resolution ct and radiologic-pathologic corre- lation," vol. 179, pp. 469–76, 06 1991.

[3] W. D. Jenkins, A. K. Matthews, A. Bailey, W. E. Zahnd, K. S. Watson, G. Mueller-Luckey, Y. Molina, D. Crumly, and J. Patera, "Rural areas are disproportionately impacted by smoking and lung cancer," *Preventive Medicine Reports*, vol. 10, pp. 200 – 203, 2018. [Online]. Available: http://www.sciencedirect.com/science/article/pii/S2211335518300494

[4] T. Kubo, Y. Ohno, D. Takenaka, M. Nishino, S. Gautam, K. Sugimura, H. U. Kauczor, and H. Hatabu, "Standard-dose vs. low-dose ct protocols in the evaluation of localized lung lesions: Capability for lesion characterizationilead study," *European Journal of Radiology Open*, vol. 3, pp. 67 – 73, 2016. [Online]. Available: http: //www.sciencedirect.com/science/article/pii/S2352047716300077

[5] Y.Lecun,L.Bottou,Y.Bengio,andP.Haffner,"Gradient-basedlearning applied to document recognition," *Proceedings of the IEEE*, vol. 86, no. 11, pp. 2278–2324, Nov 1998.

[6] A. Krizhevsky, I. Sutskever, and G. E. Hinton, "Imagenet classification with deep convolutional neural networks," pp. 1097–1105, 2012.

[7] M. D. Zeiler and R. Fergus, "Visualizing and understanding convolu- tional networks," in *Computer Vision – ECCV 2014*, D. Fleet, T. Pajdla, B. Schiele, and T. Tuytelaars, Eds. Cham: Springer International Publishing, 2014, pp. 818–833.

[8] K. Simonyan and A. Zisserman, "Very deep convolutional networks for large-scale image recognition," vol. abs/1409.1556, 2014. [Online]. Available: http://arxiv.org/abs/1409.1556

[9] C. Szegedy, W. Liu, Y. Jia, P. Sermanet, S. Reed, D. Anguelov, D. Erhan, V. Vanhoucke, and A. Rabinovich, "Going deeper with convolutions," in *2015 IEEE Conference on Computer Vision and Pattern Recognition (CVPR)*, vol. 00, June 2015, pp. 1–9. [Online]. Available: doi.ieeecomputersociety.org/10.1109/CVPR.2015.7298594

[10] C.Szegedy,V.Vanhoucke,S.Ioffe,J.Shlens,andZ.Wojna,"Rethinking the inception architecture for computer vision," in *2016 IEEE Confer- ence on Computer Vision and Pattern Recognition (CVPR)*, June 2016, pp. 2818–2826.

[11] K. He, X. Zhang, S. Ren, and J. Sun, "Deep residual learning for image recognition," *2016 IEEE Conference on Computer Vision and Pattern Recognition (CVPR)*, pp. 770–778, 2016.

[12] C. Szegedy, S. Ioffe, V. Vanhoucke, and A. A. Alemi, "Inception-v4, inception-resnet and the impact of residual connections on learning," in *AAAI*, 2017.

[13] F. Chollet, "Xception: Deep learning with depthwise separable con- volutions," *2017 IEEE Conference on Computer Vision and Pattern Recognition (CVPR)*, pp. 1800–1807, 2017.

[14] G.Huang,Z.Liu,L.v.d.Maaten,andK.Q.Weinberger,"Denselycon- nected convolutional networks," in *2017 IEEE Conference on Computer Vision and Pattern Recognition (CVPR)*, July 2017, pp. 2261–2269.

[15] B. Zoph, V. Vasudevan, J. Shlens, and Q. V. Le, "Learning transferable architectures for scalable image recognition," vol. abs/1707.07012, 2017. [Online]. Available: http://arxiv.org/abs/1707.07012

[16] M. T. Islam, M. A. Aowal, A. T. Minhaz, and K. Ashraf, "Abnormality detection and localization in chest x-rays using deep convolutional neural networks," vol. abs/1705.09850, 2017. [Online]. Available: http://arxiv.org/abs/1705.09850

[17] X. Wang, Y. Peng, L. Lu, Z. Lu, M. Bagheri, and R. M. Summers, "Chestx-ray8: Hospital-scale chest x-ray database and benchmarks on weakly-supervised classification and localization of common thorax diseases," in *The IEEE Conference on Computer Vision and Pattern Recognition (CVPR)*, July 2017.

[18] P. Rajpurkar, J. Irvin, K. Zhu, B. Yang, H. Mehta, T. Duan, D. Ding, A. Bagul, C. Langlotz, K. Shpanskaya, M. P. Lungren, and A. Y. Ng, "Chexnet: Radiologist-level pneumonia detection on chest x-rays with deep learning," vol. abs/1711.05225, 2017. [Online]. Available: http://arxiv.org/abs/1711.05225

[19] Q. Guan, Y. Huang, Z. Zhong, Z. Zheng, L. Zheng, and Y. Yang, "Diagnose like a radiologist: Attention guided convolutional neural network for thorax disease classification," vol. abs/1801.09927, 2018. [Online]. Available: http://arxiv.org/abs/1801.09927

[20] J.Shiraishi,S.Katsuragawa,J.Ikezoe,T.Matsumoto,T.Kobayashi,K.- I. Komatsu, M. Matsui, H. Fujita, Y. Kodera, and K. Doi, "Development of a digital image database for chest radiographs with and without a lung nodule: Receiver operating characteristic analysis of radiologists' detection of pulmonary nodules," vol. 174, pp. 71–4, 02 2000.

[21] O. Russakovsky, J. Deng, H. Su, J. Krause, S. Satheesh, S. Ma, Z. Huang, A. Karpathy, A. Khosla, M. S. Bernstein, A. C. Berg, and F. Li, "Imagenet large scale visual recognition challenge," vol. abs/1409.0575, 2014. [Online]. Available: http://arxiv.org/abs/1409.0575

[22] D. P. Kingma and J. Ba, "Adam: A method for stochastic optimization," vol. abs/1412.6980, 2014. [Online]. Available: http: //arxiv.org/abs/1412.6980

[23] B. Zhou, A. Khosla, A. Lapedriza, A. Oliva, and A. Torralba, "Learning deep features for discriminative localization," in *2016 IEEE Conference on Computer Vision and Pattern Recognition (CVPR)*, June 2016, pp. 2921–2929.